Research Paper

PKPD Model of Interleukin-21 Effects on Thermoregulation in Monkeys — Application and Evaluation of Stochastic Differential Equations

Rune Viig Overgaard,[1,2,3,5] Nick Holford,[4] Klaus A. Rytved,[2] and Henrik Madsen[1]

Purpose. To describe the pharmacodynamic effects of recombinant human interleukin-21 (IL-21) on core body temperature in cynomolgus monkeys using basic mechanisms of heat regulation. A major effort was devoted to compare the use of ordinary differential equations (ODEs) with stochastic differential equations (SDEs) in pharmacokinetic pharmacodynamic (PKPD) modelling.
Methods. A temperature model was formulated including circadian rhythm, metabolism, heat loss, and a thermoregulatory set-point. This model was formulated as a mixed-effects model based on SDEs using NONMEM.
Results. The effects of IL-21 were on the set-point and the circadian rhythm of metabolism. The model was able to describe a complex set of IL-21 induced phenomena, including 1) disappearance of the circadian rhythm, 2) no effect after first dose, and 3) high variability after second dose. SDEs provided a more realistic description with improved simulation properties, and further changed the model into one that could not be falsified by the autocorrelation function.
Conclusions. The IL-21 induced effects on thermoregulation in cynomolgus monkeys are explained by a biologically plausible model. The quality of the model was improved by the use of SDEs.

KEY WORDS: autocorrelation; immunomodulation; PKPD model; SDE; statistical model; thermoregulation.

INTRODUCTION

Interleukin-21 (IL-21) is a novel cytokine (1) that is produced by activated CD4^{+} T-cells and demonstrates an ability to activate CD8^{+} killer T-cells, natural killer, and B-cells (2). These immunomodulatory functions lead to the hypothesis of IL-21 as a potential anti-cancer immunotherapeutic drug, which is presently under investigation in clinical studies. Like many other anti-cancer agents, including other interleukins, IL-21 is seen to produce a broad range of biological effects that may be related to both efficacy and safety of treatment. The present work focuses on the effects of human recombinant IL-21 on thermoregulation in monkeys where IL-21 is observed to cause an increased core body temperature.

Drugs may modify the regulation of body temperature, either by changing heat production i.e., increasing metabolism, by changing heat loss e.g., by cutaneous vasoconstriction, or indirectly by changing the regulation process i.e., by increasing the set-point temperature (3) that may be associated with lowering the signalling of temperature sensitive neurons in the hypothalamus. In technical terms, fever has been defined as a state of elevated body temperature caused by an elevated thermoregulatory set-point (4). However, this definition is still under debate (5), and we shall use the term fever in the broader meaning of the word that includes any kind of hyperthermia, and refer to the specific mechanistic causes when necessary. Drug-induced fever is observed following treatment with a wide variety of drugs (3) e.g., halothane causes a hypermetabolic state called malignant hyperpyrexia, phenothiazines cause an increase in the set-point temperature, and anticholinergic drugs increase temperature by decreasing sweat production. Fever is a characteristic effect of pyrogenic cytokines, for which elevation of the set-point is a likely, but possibly not the only mechanism. Most often, fever is associated with fatigue and nausea and can significantly reduce the quality of life, while the more extreme drug induced hyperthermia can be fatal. Fever caused by an elevated set-point can be treated with antipyretic drugs, e.g., the NSAIDs, whereas hyperthermia caused by a hypermet-

[1] Informatics and Mathematical Modelling, Technical University of Denmark, Richard Petersens Plads, Building 321, Room 015, Kongens Lyngby 2800, Denmark.
[2] Novo Nordisk A/S, Copenhagen, Denmark.
[3] Department of Pharmaceutical Biosciences, Uppsala University, Uppsala, Sweden.
[4] Department of Pharmacology & Clinical Pharmacology, University of Auckland, Auckland, New Zealand.
[5] To whom correspondence should be addressed. (e-mail: ruvo@ novonordisk.com)

ABBREVIATIONS: ACF, autocorrelation function; IL-21, interleukin-21; IOV, inter-occasion variability; ODE(s), ordinary differential equation(s); PKPD, pharmacokinetic pharmacodynamic; PGE$_2$, prostaglandin E$_2$; QQ, quantile-quantile; SDE(s), stochastic differential equation(s); UR, unbound receptor.

abolic state is generally unaffected by the antipyretics and more difficult to treat.

The present work proposes to quantify interleukin-21 (IL-21) induced elevation of core body temperature in cynomolgus monkeys with a pharmacokinetic pharmacodynamic (PKPD) model. The mechanism for IL-21 induced fever are currently unknown, but they are believed to include elevated thermoregulatory set-point, consistent with the clinical finding that IL-21 induced fever can be brought down by administration of paracetamol, and with findings of other cytokines. PKPD modelling of drug induced changes in body temperature can provide a summary description of the observed effects, enable predictions for other administration schemes, and increase understanding of the underlying mechanisms. For a general system, one could imagine that modelling of temperature could forecast dangerous hyperthermia, or guide administration of antipyretic drugs given in combination with fever inducing drugs.

Modelling of the regulation and variation of body temperature are well established problems that have been challenged with many types of mathematical models. Some models incorporate a vast amount of physiological and physical details about heat regulation that enables fruitful simulation models, e.g., (6). Other more statistical models aim to precisely describe and help to identify the circadian rhythm of body temperature, e.g., see (7) and (8). PKPD models of temperature regulation are typically formulated via a system of ordinary differential equations (ODEs) incorporated in a mixed-effects model to account for inter-individual differences, e.g., see (9–11). Among these, the set-point model involves a complex systems feedback mechanism that has proven useful for several studies (10,11). Whereas these efforts have been productive, we find that previous PKPD models of temperature regulation fail to integrate many of the elements in the physiological simulation models as well as the methodology applied in more statistical models. The present model aim to comply with these two points, as discussed below.

Aspects of more physiological models has been included by extending a model with a set-point to include also metabolism and heat loss; all merged in accordance with the basic, but evidently not all theory of heat regulation and experimental findings in monkeys. This allows the pharmacodynamic effect to be described as direct effects on the metabolism, the set-point, and/or the heat conduction with a natural inclusion of the basic counter regulatory mechanisms of the body, which may improve predictions of new experimental situations. Note that this type of model aim to include the most basic mechanisms to explain the most basic phenomena of heat regulation, but we do not aim to produce a model that can explain all phenomena of this complicated system.

The methodology of more statistical temperature models is incorporated by extending the set of ODEs to a set of stochastic differential equations (SDEs), using a mixed-effects model based on SDEs (12). The use of SDEs is a novel technique in PKPD modelling that has been presented both as a diagnostic tool that can facilitate systematic model development (13,14), and also as a means to facilitate a more realistic description of the variations in the system (15,16). The present work focuses on the implementation of SDEs to provide a more realistic description of the variations, and among other things, we aim to demonstrate that implementation of SDEs may improve the predictions of the model by producing more realistic probabilities for a given animal to get fever. Since SDEs is a new technique of PKPD modelling, it will be emphasized how the results using SDEs differ from the corresponding results based on ODEs.

MATERIALS AND METHODS

The study plan was reviewed and approved by a Novo Nordisk ethical committee. The animal unit was animal welfare monitored and found to be in compliance with the Novo Nordisk Principles for the use of animals as well as national legislation and the NIH "Guide for the Care and Use of Laboratory Animals."

Animals

Sixteen purpose bred adolescent male cynomolgus primates (*Macaca fascicularis*) obtained from Guangxi, China, were used in the study. Prior to the study each primate was examined by veterinary surgeon and confirmed fit for the study.

The animals were implanted with telemetry transducers, type TL11M2-D70-PCT (Data Sciences International), for measurement of core body temperature. The animals were group-housed in a primate unit in gang cages. The room was illuminated by fluorescent lights timed to give a 12 h light–dark cycle. The temperature range was 21–26°C and the relative humidity range was 41–86%. The animals were aged 3.6 to 4.75 years and weighed 3.1–4.8 kg at the initiation of the study. The primates were fed a diet of MP(E) SQC (Special Diets Services, Witham, UK) with a supplementary diet of fruit, vegetables, and nuts. Tap water was available *ad libitum*.

The animals were acclimatized in general three weeks prior to the study and in the measuring cage on three occasions before the initiation of the study. A number of environmental enrichments were available: swings, stubs, swimming pool, puzzle feeders, toys etc.

Data Acquisition

During data acquisition the animals were in isolation cages within the animal house. Each telemetered cage was equipped with Data Sciences receivers. A Data Sciences telemetry recording system was used for continuous recording of the physiological data. The acquisition and analysis were made using Notocord HEM data acquisition and analysis software (version 3.2). For each dose, data collection commenced at least 1 h before dosing and ended approximately 24 h after dosing with 500 Hz sampling. Pretreatment of data prior to modelling involved, assessment of average temperature for each 10 min interval, keeping only the first average temperature of each hour.

Study Design

Four dosing groups consisting of four animals each were treated with 0, 0.03, 0.5 or 3 mg/kg IL-21. The animals were

dosed by intravenous bolus injection. The dose volume for the 0.5 and 3.0 mg/kg IL-21 administrations was 3.0 ml/kg and 1.0 ml/kg for the 0.03 mg/kg IL-21 administrations. The animals received a dose on days one, three and five of the study. Following each dose body temperature was recorded continuously for 24 h.

The study was conducted in accordance with the OECD Principles of GLP.

MODEL OF TEMPERATURE REGULATION

The PKPD model of temperature regulation can be divided into two parts. First, a baseline model that aims to reflect physiological mechanisms of temperature regulation, including the effects induced by a circadian rhythm, changes in ambient temperature, and/or forced changes in metabolic rate, e.g., induced by exercise. This part is presumably generally applicable for other drugs, since various pharmacological mechanisms can be implemented. The second part of the model includes a specific proposal for the pharmacodynamic effect of IL-21 on thermoregulation. For a brief overview of the structural model, see Fig. 2. The description of the inter- and intra-individual variability models are of special interest for the present analysis, and shall be described separately after presentation of the structural model.

Baseline Model

Body temperature is ultimately regulated by the balance of heat production and heat loss, where the primary mechanism of regulation is based on control of heat loss, whereas increased metabolism, e.g., by shivering is used in more extreme situations, see (17). In this setting, heat production is understood as an independent variable that drives the system, i.e., metabolism varies in order to meet the energy demand of daily living, causing changes first in temperature and subsequently in heat loss. One could imagine two ways of regulating heat loss after an increased heat production, see Fig. 1. First, the heat loss may increase to approach the metabolic rate and thus obtain heat balance, where the delay between the increase in heat production and increase in heat loss will lead to heat balance at an elevated temperature. Second, the heat loss may exceed heat production so that heat balance will not be reached until the temperature has decreased to its original baseline value.

The physiology of heat regulation reviewed in (17) indicates that heat loss is controlled to obtain balance between heat production and heat loss, rather than to defend a specific temperature. We note that temperature sensing is probably the most important mechanism to detect discrepancies between heat production and loss in order to control this balance. Experimental results lead to the understanding that the typical nocturnal decrease of body temperature is a consequence of the delay between a rapid decrease in metabolic rate e.g., due to inactivity, and the subsequent decrease in heat loss until temperature returns to a new steady state. The present model adheres to this concept by letting metabolic rate drive the circadian rhythm, and further by letting body temperature control conduction of heat. An increased heat production or equivalently an increase in external temperature will increase the body temperature, and subsequently the regulatory mechanism will increase heat conductance and thereby also heat loss, which ultimately drives the system towards steady state at a higher temperature. The equations can be written,

$$M_c(t) = \begin{cases} M_{day} & \text{for } t \in \left\{ [0, t_{night}], [t_{day}, t_{night} + 24h], ... \right\} \\ M_{night} & \text{for } t \in \left\{ [t_{night}, t_{day}], [t_{night} + 24h, t_{day} + 24h], ... \right\} \end{cases}$$
$$dM/dt = -k_m(M - M_c(t)) \quad ; \quad M(0) = M_{day}$$
$$dT/dt = c^{-1}(M - k(T - T_a)) \quad ; \quad T(0) = T_{day}$$
$$k = k_b + k_{inc}(T - T_b)$$

$$(1)$$

M is the metabolic rate, which decays with a rate constant k_m towards the metabolism dictated by the circadian rhythm $M_c(t)$, which under normal physiological conditions varies around a baseline value M_b with a day time M_{day} and a night time value M_{night}, where t_{day} and t_{night} are the times where the day and night periods start. The mechanisms causing diurnal variation in $M_c(t)$ are not included in the present model. c
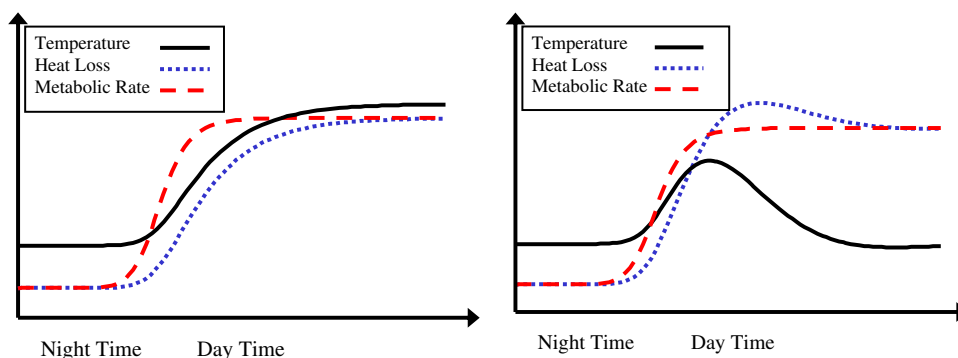

Fig. 1. Two possible ways of regulating heat loss after an increased heat production. First (*left*), the heat loss may increase to approach the metabolic rate and thus obtain heat balance, where the delay between the increase in heat production and increase in heat loss will lead to heat balance at an elevated temperature. Second (*right*), the heat loss may exceed heat production so that heat balance will not be reached until the temperature has decreased to its original baseline value.
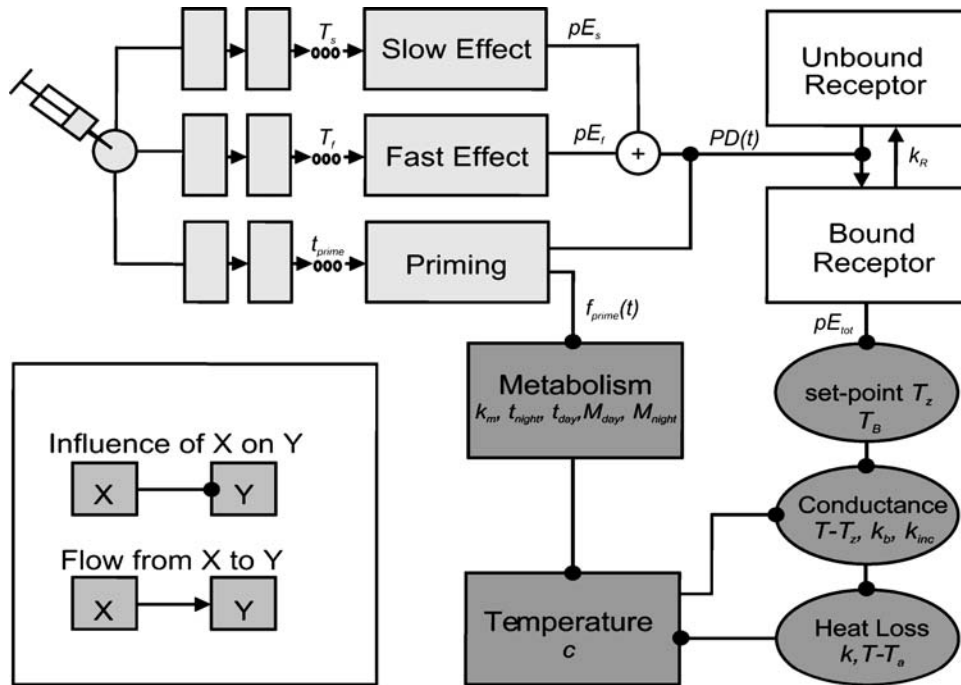
Fig. 2. Model for IL-21 induced regulation of core body temperature in cynomolgus monkeys. The model includes a part that describes the general mechanisms for temperature regulation (*dark*), a part that describes how IL-21 is believed to regulate the set-point through prostaglandin E$_2$ (*white*), and a part that empirically explains the relationship between administration of IL-21 and the effects (*light*). Each square box represents a compartment, i.e., a differential equation or the solution thereof, whereas each oval box represents an algebraic expression. A physical flow from one compartment to the next is depicted with an arrow, while a bullet is used to signify an influence of one model entity on another.

is the specific heat constant, T_a is the ambient temperature, k is the conductance of heat, which has the baseline value k_b when the temperature is at baseline T_b, and k_{inc} gives the increment in conductance per degree when the temperature rises. The model explains heat loss, only through terms proportional to the difference between body temperature and ambient temperature $(T - T_a)$, as appropriate for conduction. Radiation causes a heat loss proportional to $(T^4 - T_a^4)$ and evaporation is typically understood as temperature independent. Conductance ceases to explain heat loss for example when T_a approaches body temperature, and the model should be extended if it is needed to include e.g., high ambient temperatures.

The structural parameters to be estimated for the baseline model were chosen as: T_b, k_{inc}, k_m, t_{day}, t_{night}, and ΔT, where ΔT is the difference between day and night time steady state temperature, T_{day} and T_{night}. $T_{day} = T_b + \Delta T/2$, and $T_{night} = T_b - \Delta T/2$.

Neither the specific heat nor the baseline metabolic rate are identifiable when only temperature data is available, and consequently c was fixed to values obtained in humans, $c = 3.47$ kJ/(kg C), and M_b was fixed to 3 W/kg. This value was derived using squirrel monkey baseline metabolic rate of approximately 4 W/kg (18), and allometric scaling (19). Likewise, the ambient temperature was fixed to 21°C, as suggested by the experimental conditions, and except for k_{inc}, the model was not sensitive to changes in the ambient temperature. The baseline conductance and the night and

day time metabolic rate can now be calculated from the steady state conditions:

$$\begin{aligned}
k_b &= M_b/(T_b - T_a) \\
M_{day} &= \left(k_b + k_{inc}\left(T_{day} - T_b\right)\right)\left(T_{day} - T_a\right) \\
M_{night} &= \left(k_b + k_{inc}\left(T_{night} - T_b\right)\right)\left(T_{night} - T_a\right)
\end{aligned} \qquad (2)$$

Pharmacodynamic Model

The baseline variations of temperature regulation can be altered e.g., by disease, or by the introduction of exogenous compounds. Drugs are seen to modify thermoregulation either by directly affecting the metabolic rate, by direct effects on the heat loss, e.g., via vasodilatation, or indirectly by affecting the set-point temperature. Physiologically, the set-point is modulated through the temperature sensing neurons in the hypothalamus. If these neurons emit signals that correspond to a temperature lower than the set-point, the conductance is decreased and the temperature increases towards a higher steady state. For the baseline model described above, there is no single temperature that the body regulates towards, rather the level of the steady state temperature depend upon the metabolic rate. Consequently, it is necessary to define the set-point temperature relative to some metabolic rate. In the present work, the set-point is defined as the temperature the

body regulates itself towards at M_b, i.e., T_b if no drug has been introduced. The introduction of drugs can be understood to change the baseline model by,

$$dM/dt = -k_m(M - f_1(M_c(t), Drug, t))$$
$$dT/dt = c^{-1}(M - k(T - T_a)) \qquad (3)$$
$$k = k_b + k_{inc}(T - T_b(1 + f_3(Drug, t))) + f_2(Drug, t)$$

where f_1, f_2, and f_3, are some functions of time and drug intervention, as typically modelled via plasma concentration. f_1 allows drug modulated steady state metabolism, f_2 describes a drug effect on heat conduction, whereas f_3 involves drug modulation of the set-point to a new value $T_z = T_b(1 + f_3(Drug, t))$. Whereas this model structure can be used to describe the effects of a given drug, it is unlikely that it can be used to discriminate between e.g., effects on set-point and direct effects on conductance, when based exclusively on temperature data without precise knowledge of the function of drug effect.

The IL-21 induced rise of body temperature in cynomolgus monkeys is a rather complex set of phenomena (see data presented in Fig. 5 in the following section):

1) The effect of IL-21 seems to be absent following the first dose. This phenomenon confirms previous findings, indicating the existence of some regulating mechanism that must be switched on before any IL-21 induced effects on temperature can occur. For the 3 mg/kg treatment group, the temperature seems to be unaffected within 24 h of the first dose, but an increase is seen 48 h later at the time of the second dose. For the 0.5 mg/kg group, most monkeys exhibit only a partial response to the second dose, and a full response to the third dose.

2) The nocturnal decrease in temperature seems to vanish for the two highest treatment groups during the period where IL-21 has an effect. Note that the monkeys were unable to sleep in these periods.

3) IL-21 induces fast as well as slow temperature elevations. A quick peak is seen to last about 24 h, whereas a slower mechanism leads to persistent elevated temperature 48 h after the second dose of 3 mg/kg.

4) The fast peak is considerably lower in magnitude when temperature is already elevated; compare e.g., the effect following third dose in the 0.5 and the 3 mg/kg treatment groups.

The delayed onset of the pharmacodynamic effects (phenomenon 1) was modelled with an empirical function that starts at 0 indicating no effect, and when the time since the first dose increases, the function smoothly goes towards one, indicating full effect. We assume that a certain dose level is necessary for this priming to take place, but the available data did not allow a reasonable estimate of this value. For practical reasons, priming was implemented only for the high dosing groups, where an effect on temperature was seen in the animals. The following priming function was used,

$$f_{prime}(t) = \delta_{high\_dose}(1 - \exp(-\alpha(t - t_{dose1} - t_{prime})))^{-1} \quad (4)$$

where δ_{high_dose} is 0 for the low dose levels and 1 for the high dose levels, t_{dose1} is the time of administration of dose 1, t_{prime}

is the characteristic time of priming, and α gives the shape of the priming function. The priming function for the onset of the pharmacodynamic effect was also used to model the disappearance of the nocturnal decrease in the metabolic rate (phenomenon 2). This effect on metabolism, perhaps by preventing sleep and rest at night, was consistent with simultaneous observations of heart rate that maintain a day time high value during nights when IL-21 affects temperature, but exhibit a nocturnal decrease when no effect is seen on temperature. The steady-state day and night time metabolic rates were modelled to be changed by the drug as

$$M_{day}^* = f_1(Drug, t)_{day} = M_{day}$$
$$M_{night}^* = f_1(Drug, t)_{night} = (1 - f_{prime})M_{night} + f_{prime}M_{day}$$
$$(5)$$

where M_{day}^* and M_{night}^* are the drug modulated day and night time metabolic rates. At the present time, we were not able to formulate a reasonable model for "un-priming" of the system, e.g., the return to a normal circadian rhythm. It may be appropriate to develop more realistic and mechanistic dose-response relationships for the priming and the "un-priming," but at present we use the function given above.

The fast and slow effects following dosing with IL-21 (phenomenon 3) are modelled to elevate the thermoregulatory set-point as described below. Both effects are described by gamma distribution functions giving the solution to a system of transit compartments that could represent the chain of events between dosing and effect. The gamma distribution function can be written as

$$g_{N,T}(t) = \exp(-tN/T)(t)^{N-1}(N/T)^N(N-1)! \text{ for } t$$
$$> 0; g_{N,T}(t) = 0 \text{ for } t \leq 0 \quad (6)$$

where g_{NT} is the gamma function, yielding the value in the Nth transit compartment, and T is the mean total transit time to compartment N. In the model, the slow effect is dose proportional, whereas the fast effect is a dose independent fixed response. Such dose independence could reflect that the maximum effect has been reached, or that a predetermined acute phase response is induced. The total effect is modelled as the sum of the slow and the fast effect, and proportional to the priming function, which ensures that the effect is seen only when the priming has occurred. The equations describing these rather empirical effects are,

$$E_{slow} = pE_s \sum_{doses} AMT_{doses}g_{Ns,Ts}(t - t_{dose})$$
$$E_{fast} = pE_f \sum_{doses} g_{Nf,Tf}(t - t_{dose}) \quad (7)$$
$$PD(t) = f_{prime}(t)(E_{slow} + E_{fast})$$

where AMT_{dose}. is the amount of IL-21 administered by a given dose at time t_{dose}. The mean total delay for the slow and the fast effect is parameterized by T_s and T_f, whereas pE_f and pE_s gives the level of the fast and the slow effect. N_f and N_s are the number of transit compartments used in the two effects, both fixed to four in order to produce a standard third order delay between the dose and the effect compart-

ment. It was judged reasonable to combine the fast and the slow effect, assuming that they act through the same mechanism, as motivated by the observed saturation of the combined effect (phenomenon 4). The combined pharmacodynamic effect PD(t) is modelled to affect the thermoregulatory set-point. Although not completely understood, this effect is likely mediated by prostaglandin E_2 (PGE$_2$), which is believed to mediate cytokine induced fever (20–22) by lowering the signalling of temperature sensitive neurons in the hypothalamus. Many possible mechanisms can be proposed to describe the link between drug effect, PGE$_2$ release, and the subsequent increase in set-point temperature. A simple E_{max} model could describe the set-point temperature as a saturable function of PD(t). In general the E_{max} relationship can be motivated by the classical receptor occupancy theory under the assumption of equilibrium, e.g., see (23). However, for the present analysis, this receptor occupancy was modelled explicitly, without the assumption of steady state. The rate of increase in the number of bound receptors is proportional to the pharmacodynamic effect and the fraction of unbound receptors. When no pharmacodynamic effect is present, the bound receptors will decay to unbound receptors. This can give rise to phenomenon four—saturation in effect, because for an elevated temperature, only few unbound receptors will be available, so a subsequent response will produce only a few more bound receptors. We get,

$$dBR/dt = PD(t)(1 - BR) - k_R BR \quad ; BR(0) = 0$$
$$f_3(Drug, t) = pE_{tot}BR \quad ; \; T_z = (1 + pE_{tot}BR)T_b \tag{8}$$

BR is the fraction of bound receptors, and k_R is the off rate. Empirically, k_R give us one extra parameter to describe the shape of the delayed fast and slow effects, and further for the SDE model k_R is also involved in the correlation structure for the residuals, to be discussed below. The actual effect on the set-point is proportional to the fraction of bound receptors with the coefficient being the effect parameter pE_{tot}. Whereas, pE_f and pE_s parameterize the effect on the receptors, i.e., they control the induced level of saturation. The complete set of structural parameters to be estimated for the pharmacodynamic model was chosen as: (pE_{tot}, k_R, t_{prime}, T_s, T_f, pE_f, pE_s, and α).

The complete model of the mechanistic baseline system, the mechanistic effect model, and the empirical drug interaction are presented in Fig. 2, while simulations of the different model entities are presented in Fig. 3. Following the first administration of IL-21, the system will become primed according to Eq. (4), which will affect the metabolic rate to maintain a day time value Eq. (5). Subsequent administrations of IL-21 will exhibit a reduced or a full response Eq. (7), where the fast effect is of a fixed size, whereas the slow effect is proportional to the dose level. The effect will convert unbound receptors to bound receptors Eq. (8), which raises the thermoregulatory set-point Eq. (8), so that the normal physiological regulatory system will raise the body temperature according to the change in set-point and metabolic rate, see Eq. (3) or Eq. (9).

Variability Model

The present analysis utilize a new technique for variability in PKPD models, where system noise is added to a set

of ordinary differential equations to account for model mis-specification and true random fluctuations, producing a set of stochastic differential equations. The SDEs are embedded into a typical mixed effects setting with uncorrelated measurement noise and inter-individual and/or inter-occasion variability in the parameters. In summary, the intra-individual statistical model can be written as,

$$dM = -k_m(M - f_1(Drug, t))dt + \sigma_M dW_M \quad ; \; M(0) = M_{day}$$
$$dT = c^{-1}(M - k(T - T_a))dt \quad ; \; T(0) = T_{day}$$
$$dBR = (PD(t)(1 - BR) - k_R BR)dt + \sigma_{BR}dW_{BR} \quad ; \; BR(0) = 0$$
$$k = k_b + k_{inc}(T - T_z) \text{ and } T_z = (1 + pE_{tot}BR)T_b$$
$$T_{obs} = T + e \quad ; \; e \in N(0, \sigma_e^2) \tag{9}$$

The SDEs given by the first three equations correspond to the ODEs previously defined, now with system noise added to the metabolism and the receptor compartment. T_{obs} gives the observed temperature, modelled with additive uncorrelated measurement noise e, which is normally distributed with standard deviation σ_e. $\sigma_M dW_M$ and $\sigma_{BR}dW_{BR}$ give system noise in the metabolism and the receptor compartment, respectively. Where W_M and W_{BR} are independent standard Wiener processes, e.g., see (24). System noise produces fluctuations directly into the structural model, and will therefore depend upon the structural parameters. Specifically, the metabolism fluctuates and the correlation between the metabolic rate at time t_1 and t_2 will be $\exp(-k_m|t_1 - t_2|)$. Similarly, the correlation of BR will be $\exp(-k_R|t_1 - t_2|)$ when no drug is included. These fluctuations will thus give two time scales for the correlations in the model.

From data presented in Fig. 5, variability is seen to be higher after second dose than after third dose. This effect can be understood as inter-individual variability in the time point where the effects are switched on t_{prime}, so that the system can be more or less turned on during the second dosing day, whereas it is completely turned on for the third dose. A proportional inter-individual model was implemented as,

$$t_{prime} = \theta \exp(\eta); \; \eta \in N(0, \Omega) \tag{10}$$

where θ is the typical value of t_{prime}, and η is a normally distributed random effect with variance Ω. Several other inter-individual and inter-occasion models were investigated during model development.

MODEL DEVELOPMENT

Different models were discriminated based on, robustness, likelihood function value, reasonable physiological values of the parameter estimates, and performance of the simple predictive check described in the results.

A number of different baseline models have been investigated and rejected in favour of the chosen model. These include, square wave metabolism, sine wave metabolism, modelling temperature directly as a sine wave, and modelling heat loss to approach metabolism exponentially
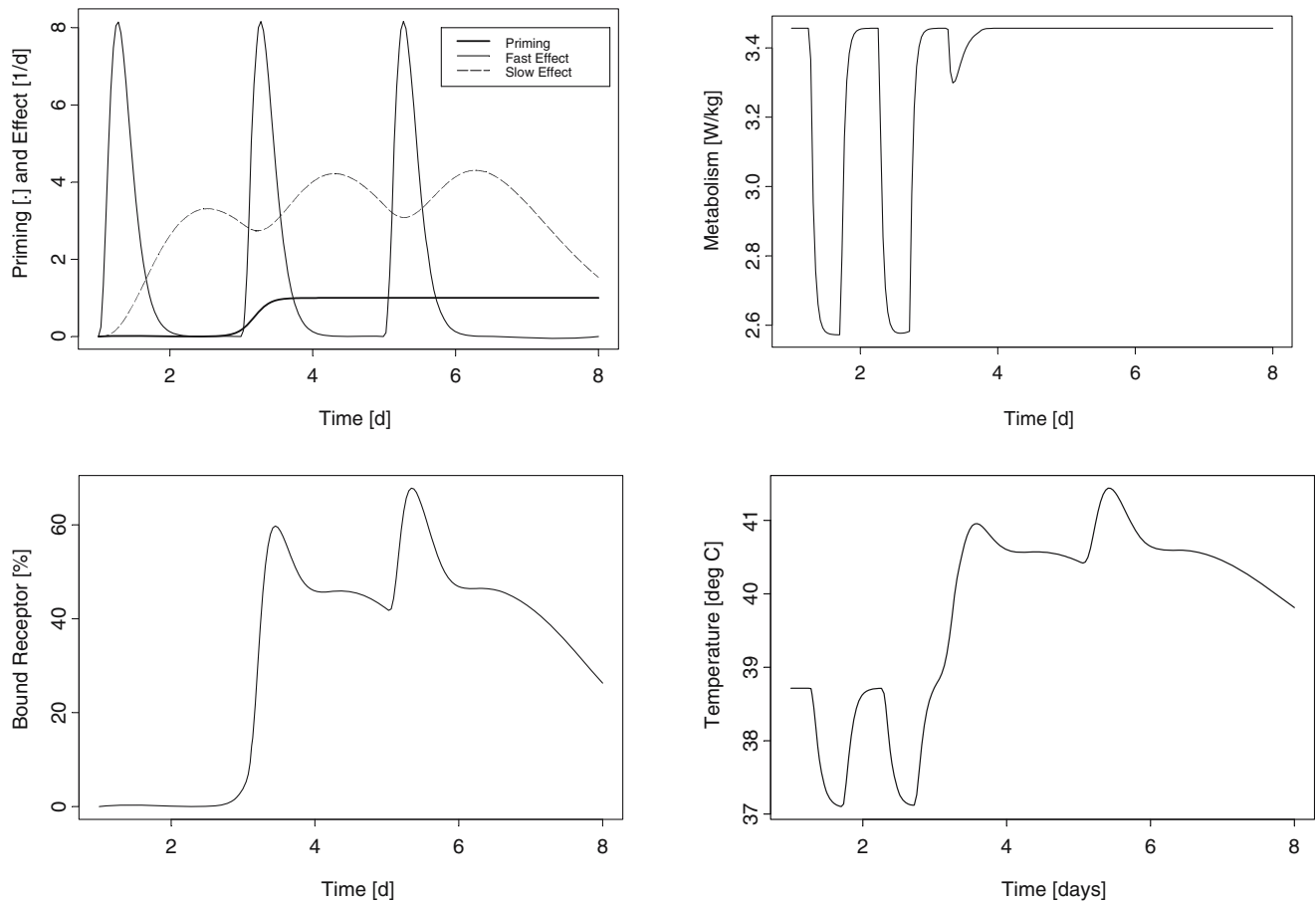
Fig. 3. Simulations of the different components in the pharmacodynamic model for IL-21 induced regulation of core body temperature in cynomolgus monkeys. These simulations illustrate the dynamics of the structural model following administration of 3 mg/kg IL-21 at days one, three, and five. The fast, the slow, and the priming effect are seen in the top left plot. After the system is primed, the metabolic rate maintains a daytime high (*top right*), and the sum of the fast and the slow effect initiates the conversion of unbound to bound receptors (*bottom left*). The bound receptors elevate the set-point, giving rise to an elevated temperature (*bottom right*).

instead of the chosen model where change in conductance gives the change in heat loss. It was not tested whether a more complicated oscillator model, as e.g., described in (25), could explain the circadian rhythm.

During development of the pharmacodynamic model, it was investigated whether simulated pharmacokinetic profiles could be used instead of dosing to drive the pharmacodynamics, but using dose directly turned out to be more productive. It was further investigated whether the slow and fast effects could be joined into one effect, and also whether the effect on metabolism could be explained as a function of the slow effect.

Inter-individual variability was tested for all parameters. Whereas many of these parameters were significant based on objective function value, only inter-individual variation for t_{prime} gave a large improvement, and was crucial for the performance of the simple predictive check.

Stochastic Model Development

Investigation of system noise may be motivated by the significantly autocorrelated residuals of the ODE model, as

demonstrated in Fig. 4. If the system noise parameters σ_M and σ_{BR} in the SDE model are set to zero, then we get our original ODE model. In other words, the ODE and SDE models are nested, making it appropriate to test the inclusion of system noise with the likelihood ratio test. The inclusion of system noise was highly significant with $\Delta \log(L) > 1{,}000$.

System noise was investigated for temperature, metabolism, and receptor compartments, testing also a term proportional to PD(t) in the receptor compartment. The following considerations contributed to the chosen implementation:

Stochastic fluctuations in metabolism were motivated by the natural variations in movement and exercise patterns. A simulation test confirmed that the level of fluctuations in metabolism were reasonable compared to those observed in squirrel monkeys (18). The simulations of metabolism were far from zero, and subsequently it was judged unnecessary to investigate a numerically more complicated proportional model that would ensure metabolism to be strictly positive.

System noise for the temperature compartment could to a large extent compensate for variations in metabolism, but
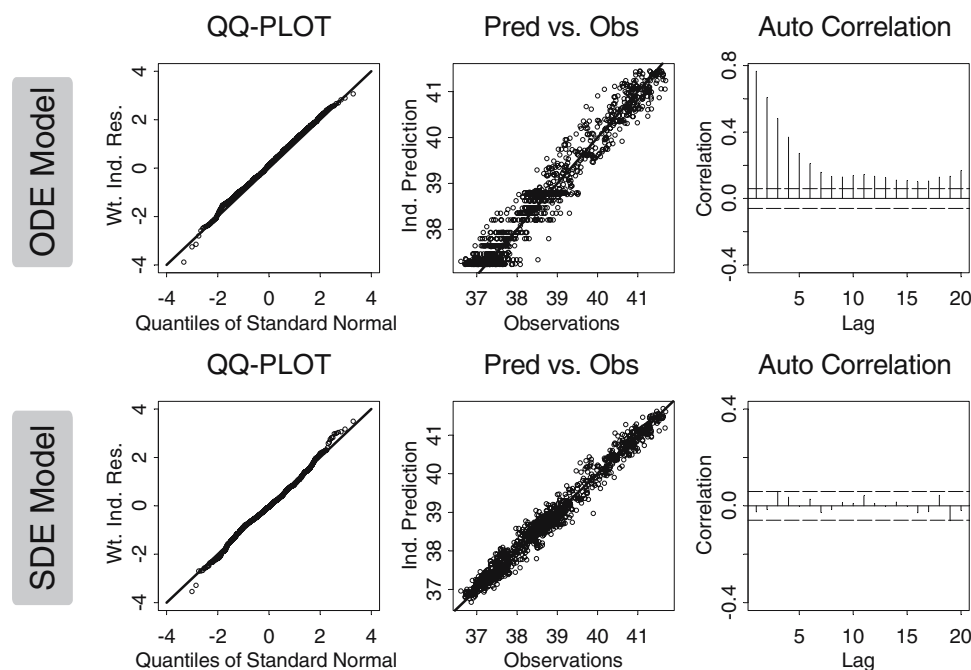
Fig. 4. Diagnostic plots for the ODE and SDE model for IL-21 induced regulation of core body temperature in cynomolgus monkeys. QQ-plots (*left*) provide a visual test for weighted individual residuals being standard normal distributed. Predicted *versus* observed plots (*middle*) are based on individual one-step predictions, which are identical to the usual individual predictions for the ODE model. The autocorrelation functions (*right*) of the weighted residuals are plotted with the 95% confidence intervals for the null hypothesis that these are uncorrelated.

including both effects gave only modest improvement to the objective function value. System noise on metabolism was selected instead of direct effects on temperature because of an improved objective function value, more realistic simulations of metabolism, and since it enabled estimation of the rate constant k_m.

System noise was also introduced for the receptor compartment, which could reasonably account for slow fluctuations and were significant in a likelihood ratio test. The chosen stochastic implementation ensures that the total number of bound and unbound receptors remain constant. A term with system noise proportional to the pharmacodynamic effect was tested and rejected.

COMPUTATIONS

Parameter estimation was performed using NONMEM (26), where stochastic differential equations were implemented in NONMEM version VI beta as explained in (14). The model was processed at the cluster of the PKPD group at Uppsala University, which is a heterogenic cluster of 20 computers with dual processors running Redhat 9 (http://www.redhat.com), kernel version 2.4.26 with the openmosix cluster patch version 2.4.26-1 (http://www.openmosix.org). To save computational time, it was chosen to estimate parameters by the following two stage procedure. First, we estimate the parameters in the baseline model, using data from the vehicle group and the 0.03 mg/kg group where no effect is seen. Second, the complete dataset is used to

estimate the pharmacodynamic parameters, including all variability parameters, while keeping baseline parameters fixed to the previously estimated values. For both steps, estimation of standard errors (SE) was obtained by bootstrapping, i.e., from the estimation results of 100 randomly generated datasets. New datasets were generated by replacing each monkey in the dataset with a randomly selected monkey, while allowing for duplicates. For bootstrapping of the pharmacodynamic model, new datasets were constrained to contain four monkeys from all of the four treatment groups.

RESULTS

Parameter estimates and their relative standard errors for the pharmacodynamic model of IL-21 induced effects on temperature regulation are presented in Table I. SDE model parameter estimates are compared to the corresponding estimates obtained with ODEs. We note that the ODE model estimate of k_m was very unstable, as indicated by a large relative standard error. During estimation of the remaining parameters, the ODE model k_m was fixed to the value obtained in the SDE model, allowing a more reasonable comparison of the two sets of estimates. For most parameters, the estimates are very similar, while some estimates clearly differ in the two estimation procedures. The most characteristic changes are that the SDE model produces estimates with lower inter-individual variability and measurement noise compared to the ODE model.

Table I. Parameter Estimates and Their Relative Standard Errors From the Model of IL-21 Induced Regulation of Core Body Temperature in Cynomolgus Monkeys

Parameter	Unit	SDE parameter estimate	ODE parameter estimate	% Difference of ODE estimate
Baseline parameters				
t_{night}	h	6.64 (1.9%)	6.73 (1.7%)	1.4
t_{day}	h	17.3 (0.8%)	17.5 (1.4%)	1.1
k_m	1/d	27.3 (17%)	*591 (140%)	2064
k_{inc}	W/(kg°C^2)	0.0169 (19%)	0.0258 (10%)	52
ΔT	°C	1.66 (3.2%)	1.57 (3.3%)	−5.4
T_B	°C	37.9 (0.15%)	38 (0.15%)	0.26
Pharmacodynamic parameters				
T_s	d	2.15 (21%)	2.45 (12%)	14.0
T_f	d	0.303 (8.4%)	0.368 (7.4%)	21.5
pE_s	kg/(d mg)	2.97 (19%)	3.57 (48%)	20.2
pE_f	1/d	2.16 (22%)	2.43 (40%)	12.5
pE_{tot}	1	0.16 (9.4%)	0.144 (10%)	−10.0
k_R	1/d	4.1 (20%)	5.35 (36%)	30.5
t_{prime}	d	2.12 (9.3%)	1.88 (16%)	−11.3
α	–	11.2 (37%)	5.35 (47%)	−52.2
Inter-individual variability				
CV(t_{prime}) η	%	14.9 (46.5%)	37.5 (37%)	152
Measurement noise				
σ_e	°C	0.102 (8.2%)	0.31 (3.9%)	224
System noise				
σ_m	W/(kgd$^{1/2}$)	1.46 (22%)	–	–
σ_R	1/d$^{1/2}$	0.179 (34%)	–	–

*For the ODE model, k_m could not be estimated reliably, and was subsequently fixed to the value estimated in the SDE model, allowing a more reasonable comparison of the remaining estimates.
The parameter estimates are compared to the corresponding model based on ordinary differential equations.
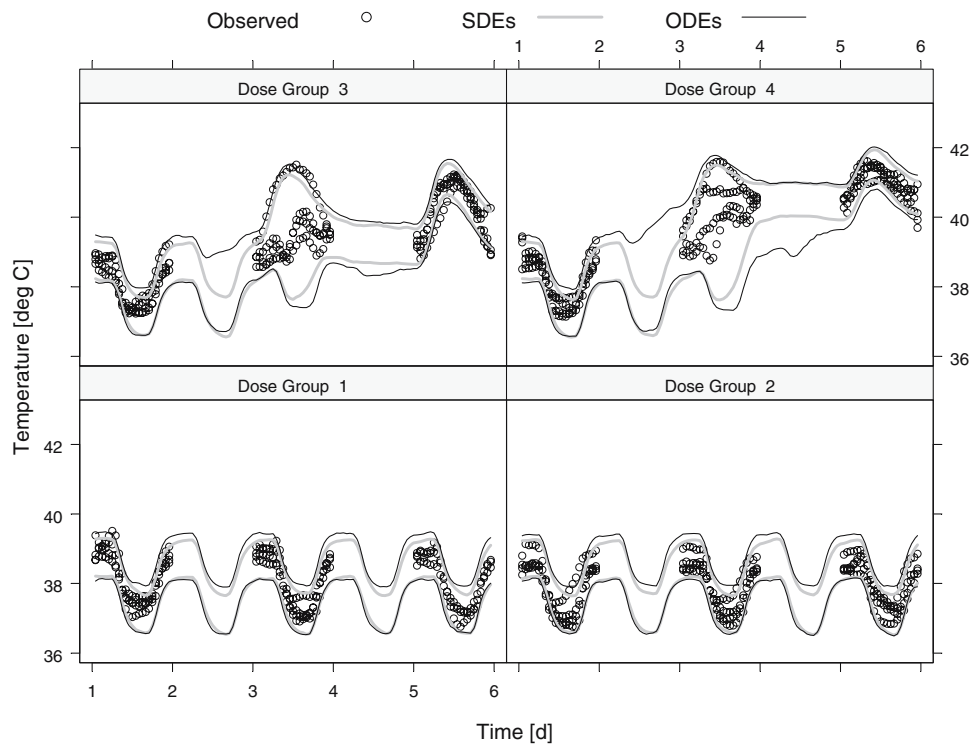

Fig. 5. 90% prediction intervals from the ODE (*thin dark*) and SDE model (*fat light*) are compared to the observed temperature (*black circles*) in four different treatment groups. Each group include four cynomolgus monkeys receiving an IV bolus administration of IL-21 at day one, day three, and day five, at a dose level of, 0 mg/kg in Group one, 0.03 mg/kg in Group two, 0.5 mg/kg in Group three, and 3 mg/kg in Group four.

A representative set of diagnostic plots are presented in Fig. 4. Similarly to the QQ-plot and the predicted *versus* observed, the autocorrelation function for individual weighted residuals was computed from the vector containing data from all individuals, as given by the NONMEM output file.

A simple predictive performance check was performed by simulating the model 500 times and calculating the 90% prediction interval. These prediction intervals were calculated both for the ODE and the SDE model and compared to the observed temperatures for each of the four treatment groups in Fig. 5. The ODE and SDE intervals are reasonably similar, with the same strengths and weaknesses. Both models capture the particularly high variability following second dose, as well as the four phenomena of the structural model: 1) absent effect after first dose, 2) effects on temperature circadian rhythm, 3) fast and slow effects, and 4) saturation of effect. The 90% prediction intervals seem to include more than 90% of data, which indicates a slightly overestimated variation, more so for the ODE model than the SDE model.

Figure 6 compares simulated individual profiles from the SDE model and the ODE model of the observed temperatures following third administration of IL-21 at a dose level of 3 mg/kg, which is the most critical time for the present study. Simulations based on SDEs vary continuously, similarly to the observed temperatures, whereas ODE simulations are seen to jump up and down erratically.

DISCUSSION

The thermoregulatory effects of IL-21 in cynomolgus monkeys were described by a PKPD model based on stochastic differential equations. Whereas temperature modelling is well established in the literature, the present model and results do include a series of features that justify further discussion.

Priming The mechanism behind an absent effect on temperature after first dose is presently not understood. This priming effect was described by an empirical function that switches on sometime after the first dose, and inter-individual variation in the time of onset could describe an increased variation after second dose. However, the model does not satisfactorily describe how the system returns to normal. During model development it was attempted to model priming as a function of the slow effect, but various attempts were discarded because of poor simulation properties.

Receptor model The standard E_{max} model was extended to explicitly include a receptor compartment, extending the model with an off rate for the receptors k_R. Empirically, this off rate is related to the shape of the response, and to the correlation structure in the SDE model. The estimated value for k_R corresponds to a half-life of 4 h, and it is presently not known whether this off rate relate to that of any physiological receptor involved in the response. In particular, intracerebral injections of PGE_2 in rat leads to elevated temperatures lasting for only tens of minutes (22), indicating a much faster half life of response.

Metabolism model Whereas the metabolism was unobserved in the present study, the circadian rhythm of thermoregulation has been investigated in detail for squirrel monkeys (18). These calorimetric experiments showed that the metabolic rate begin to decrease around the time of lights-off, and reach a stable level within 1.5–2.5 h. This is in reasonable agreement with the estimated value of k_m, corresponding to a half life of 0.7 h for cynomolgus monkeys. Since the correlation structure in data contributed significantly to the estimation of k_m, this result constitutes a test, both for the structural model and for the implemented system noise.

For the squirrel monkeys, it was also found experimentally that the metabolic rate varies approximately between 3 W/kg at night and 5 W/kg at day (18). Cynomolgus monkeys are approximately three times larger than squirrel monkeys, so allometric scaling yield a night and day time metabolic rate, of 2.57 and 3.45 W/kg in cynomolgus monkeys. In the present analysis, we used a fixed baseline metabolic rate M_b in cynomolgus monkeys of 3 W/kg. From the fixed value of M_b and the estimated parameter values of k_{inc}, T_b, and ΔT, we can calculate or simulate model predictions for the night and day time metabolic rate in cynomolgus monkeys. The model prediction yield night and day time values at 2.63 and 3.40 W/kg which is in perfect agreement with the values found by allometric scaling.

Model Diagnostics A series of diagnostic plots were presented in Fig. 4 to compare the ODE model with the SDE model. Models based on ODEs typically assume independence of the individual prediction errors, whereas SDE models assume independence of the individual one-step prediction errors, i.e., prediction errors based on predictions that include information of all previous data to predict the next observation. So the individual residuals refer to the one-step prediction errors, which reduce to the usual prediction errors when
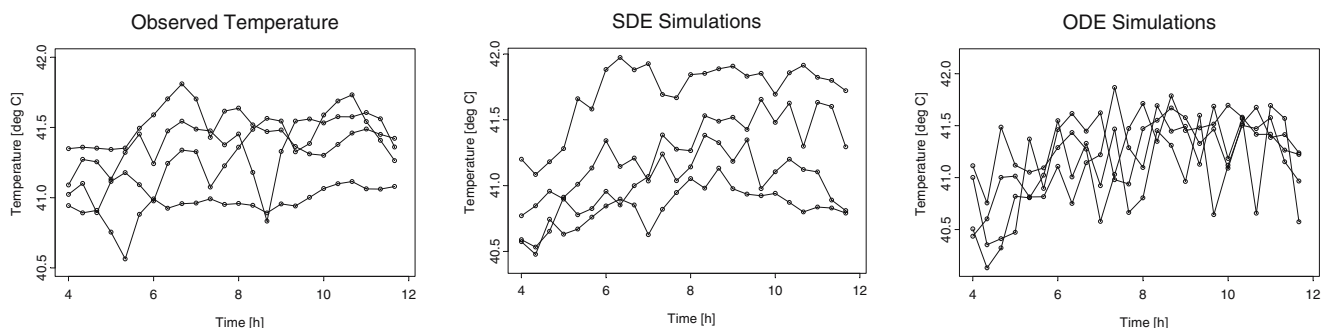

Fig. 6. Core body temperature for cynomolgus monkeys 4 h to 12 h post third administration of IL-21 at a dose level of 3 mg/kg. The three plots compare the actual observed temperatures for the four monkeys (*left*) to simulations of four monkeys based on the SDE model (*middle*) and the ODE model (*right*).

ODEs are used. Diagnostic plots of predictions *versus* observations demonstrate that SDE model predictions are closer to the observations than ODE model predictions, illustrating that one-step predictions are based on all previous data for SDEs, but not for ODEs. The autocorrelation function presented in Fig. 4 clearly demonstrates significantly correlated individual residuals for the ODE model, which falsifies the statistical model assumption. The SDE model on the other hand, successfully passes this statistical test. Diagnostic Quantile–Quantile (QQ) plots presented in Fig. 4 illustrate that the weighted individual residuals are close to being normal distributed for the SDE model as well as for the ODE model. This is one of the fundamental assumptions for both models, and particularly for the Extended Kalman Filter approximation to the individual SDE likelihood function (12). Failure to produce Gaussian residuals may indicate that the Extended Kalman Filter is inadequate, possibly motivating the pursuit of higher order filters or other estimation methods (24).

Do SDEs represent true fluctuations? Investigation of system noise may be motivated by the significantly autocorrelated residuals of the ODE model, as demonstrated in Fig. 4. Such correlations may be due to true variations that can be modelled by SDEs, or by model misspecification that may be described but not reproduced by SDEs. If the estimated system noise in reality originates from model misspecification, one would presume that simulations with SDEs would produce large confidence bands, because unlike a model deficiency, system noise will change the model in a different direction with every simulation. Figure 5 clearly demonstrates that the SDE model reproduces data with reasonable confidence bands, leading to the conclusion that the autocorrelated residuals reflect true fluctuations in data, and Fig. 6 confirms that the simulations look reasonable compared to data.

System noise and inter-occasion variability From a mixed-effects modelling perspective, the inter-occasion variability (IOV) and the residual variability are treated as separate entities. However, in some cases it may be more realistic to explain inter-occasion variability as a continuous random varying process, i.e., system noise that is high on some occasions and low on others. During model development, the likelihood ratio test indicated the significant between-day variability in the steady state day and night time temperature (T_{day} and T_{night}) for both the ODE and the SDE model. However, for the ODE model IOV was seen to give individual predictions that were visibly closer to data, while this was not the case for SDEs. For SDEs, IOV did not visibly improve individual predictions, neither for the diagnostic plots in Fig. 4, nor when comparing to observations over time. Since the implemented system noise seemed to reasonably describe the day-to-day variation of T_{day} and T_{night}, no explicit IOV was included for these parameters, which considerably reduced the computational time.

Simulation Properties The simple predictive check given in Fig. 5 provide a reasonable diagnostic for the model to capture overall differences between treatment groups, and thereby predict the overall outcome of new experimental designs. However, PKPD models are quite often used for predictions of new individuals possibly in new treatment regimens. For any drug that may elevate body temperature, one might be interested in the probability for a new individual to show three readings (at least 1 h apart) higher than 38°C (100.4°F) or a single reading higher than 38.3°C (101°F), which is used in oncology practice as a criteria for significant fever (27). Model predictions of such probabilities require accurate simulations of the individual profiles. Figure 6 demonstrate that simulations based on SDEs vary continuously, similarly to the observed temperatures, whereas ODE simulations are seen to jump up and down erratically, possibly leading to erroneous conclusions.

Benefits of SDEs In summary, the benefits of SDEs were found to include,

1. The ODE model with uncorrelated residuals could be falsified by a simple statistical test of the autocorrelation function (ACF), whereas the SDE model was able to describe the correlation structure in the residuals. The ACF can be seen as a general model diagnostic, where an erroneous ACF will falsify the model, but the ACF may also be a more direct quality mark for model simulations. In particular, simulated data could be used to assess precision of parameter estimates for different sampling schedules. It is to be expected that the results would change if simulations are made with a model that produce a completely different ACF for the residual errors.

2. The introduction of SDEs allows us to quantify and propose a mechanism for the fluctuations in temperature, i.e., random fluctuations in metabolic rate and in the fraction of bound receptors that affect the thermoregulatory set-point.

3. The high measurement error estimated in the ODE model caused simulations to jump up and down erratically and unrealistically compared to simulations based on SDEs that realistically resembled the variations seen in data. This could become important, e.g., if one wish to predict the probability that treatment of a given individual cause temperature elevation above a certain level.

4. IIV was reduced by the inclusion of system noise, and the simple predictive check demonstrated that the SDE model led to narrower confidence intervals, as is often seen with more accurate variability models.

5. SDEs allowed us to simplify the model for inter-occasion variability on day and night time steady state temperature, which significantly improved the model speed.

Other statistical techniques, such as the autoregressive (AR) process that has previously been incorporated in NONMEM (28) or the more general autoregressive moving average (ARMA) process, would also enable quite general inclusion of correlated residuals. The present approach favours SDEs, because they incorporate random fluctuations directly on the different mechanisms or entities of the model, which gives us an understanding of the origin of the correlation structure found in data.

Model Limitations and potential future applications First of all, the model includes only the most basic mechanisms of heat control, and it fail to explain what happens e.g., if the ambient temperature is changed far from 21°C.

As previously mentioned the empirical effects on priming have not been implemented to return to normal. This poses serious problems for the model to simulate longer dosing intervals, long term treatment, and termination of treatment. We should note that previous unpublished experiments have demonstrated qualitatively similar patterns of IL-21 induced effects on temperature regulation for a series of different

dosing regiments. However, the empirical parts of the model must be extended if it is to give a complete understanding of the effects of IL-21 on thermoregulation.

On the other hand, a mechanistic framework of thermoregulation has been put forward. It is hoped that this framework can be used to improve the descriptions and predictions not only for IL-21, but also for other pharmaceutical and biological compounds. In particular it is hoped that the mechanistic aspects of the thermoregulation model can improve predictions of the overall outcome of new dosing regimens, whereas the inclusion of SDEs can provide better predictions of the variations seen in temperature for individual animals.

CONCLUSION

A new baseline PKPD model for thermoregulation has been formulated to include potential effects on the circadian rhythm, metabolism, heat loss, and a thermoregulatory set-point. The baseline model quantitatively reproduces basic physiological findings of the circadian regulation of heat production and heat loss in monkeys. It further qualitatively reflects some basic effects of thermoregulation following exercise and changed ambient temperatures, while clearly not explaining all phenomena in this complicated system.

The proposed mechanisms of IL-21 were incorporated into the baseline model via effects on the circadian rhythm of metabolism, and on the thermoregulatory set-point, which could describe a complex set of IL-21 induced phenomena. These phenomena include 1) absent effect after first dose, 2) disappearance of the circadian rhythm, 3) fast and slow effects, and 4) saturation of effect. Further more, inter-individual variability in the onset of effect could explain increased variability after second dose.

System noise was implemented in the metabolism and the receptor compartment, converting the ODE model into an SDE model. SDEs provided a more realistic description of the variability that improved individual simulation/predictive properties, accelerated model speed by simplifying inter-occasion variability, and finally changed the model into one that could not be falsified by the autocorrelation function.

REFERENCES

1. J. Parrish-Novak, S. R. Dillon, A. Nelson, A. Hammond, C. Sprecher, J. A. Gross, J. Johnston, K. Madden, W. Xu, J. West, S. Schrader, S. Burkhead, M. Heipel, C. Brandt, J. L. Kuijper, J. Kramer, D. Conklin, S. R. Presnell, J. Berry, F. Shiota, S. Bort, K. Hambly, S. Mudri, C. Clegg, M. Moore, F. J. Grant, C. Lofton-Day, T. Gilbert, F. Rayond, A. Ching, L. Yao, D. Smith, P. Webster, T. Whitmore, M. Maurer, K. Kaushansky, R. D. Holly, and D. Foster. Interleukin 21 and its receptor are involved in NK cell expansion and regulation of lymphocyte function. *Nature* **408**:57–63 (2000).
2. T. Habib, A. Nelson, and K. Kaushansky. IL-21: A novel IL-2-family lymphokine that modulates B, T, and natural killer cell responses. *J. Allergy Clin. Immunol.* **112**:1033–1045 (2003).
3. P. A. Mackowiak. Drug induced fever: In fever. *Basic Mechanisms and Management*. Raven Pr. 1997.
4. T. C. Chan, S. D. Evans, and R. F. Clark. Drug-induced hyperthermia. *Crit. Care Clin.* **13**:785–808 (1997).
5. A. A. Romanovsky. Do fever and anapyrexia exist? Analysis of set point-based definitions. *Am. J. Physiol. Lung Cell. Mol. Physiol.* **287**:R992–R995 (2004).
6. G. Havenith. Individualized model of human thermoregulation for the simulation of heat stress response. *J. Appl. Physiol.* **90**:1943–1954 (2001).
7. E. N. Brown, Y. Choe, H. Luithardt, and C. A. Czeisler. A statistical model of the human core-temperature circadian rhythm. *Am. J. Physiol. Endocrinol. Metab.* **279**:E669–E683 (2000).
8. R. A. Irizarry, C. Tankersley, R. Frank, and S. Flanders. Assessing homeostasis through circadian patterns. *Biometrics* **57**:1228–1237 (2001).
9. I. F. Troconiz, S. Armenteros, M. V. Planelles, J. Benitez, R. Calvo, and R. Dominguez. Pharmacokinetic–Pharmacodynamic Modelling of the antipyretic effect of two oral formulations of ibuprofen. *Clin. Pharmacokinet.* **38**:505–518 (2000).
10. S. A. Visser, B. Sallstrom, T. Forsberg, L. A. Peletier, and J. Gabrielsson. Modeling drug- and system-related changes in body temperature: application to clomethiazole-induced hypothermia, long-lasting tolerance development, and circadian rhythm in rats. *J. Pharmacol. Exp. Ther.* (2005).
11. K. P. Zuideveld, H. J. Maas, N. Treijtel, J. Hulshof, P. H.van der Graaf, L. A. Peletier, and M. Danhof. A set-point model with oscillatory behavior predicts the time course of 8-OH-DPAT-induced hypothermia. *Am. J. Physiol. Regul. Integr. Comp. Physiol.* **281**:R2059–R2071 (2001).
12. R. V. Overgaard, N. Jonsson, C. W. Tornøe, and H. Madsen. Non-linear mixed-effects models with stochastic differential equations: implementation of an estimation algorithm. *J. Pharmacokinet. Pharmacodyn.* **32**:85–107 (2005).
13. N. R. Kristensen, H. Madsen, and S. H. Ingwersen. Using stochastic differential equations for PK/PD model development. *J. Pharmacokinet. Pharmacodyn.* **32**:109–141 (2005).
14. C. W. Tornoe, R. V. Overgaard, H. Agerso, H. A. Nielsen, H. Madsen, and E. N. Jonsson. Stochastic differential equations in NONMEM: implementation, application, and comparison with ordinary differential equations. *Pharm. Res.* **22**:1247–1258 (2005).
15. K. E. Andersen and M. Hojbjerre. A population-based Bayesian approach to the minimal model of glucose and insulin homeostasis. *Stat. Med.* **24**:2381–2400 (2005).
16. S. Ditlevsen and A. de Gaetano. Stochastic *vs.* deterministic uptake of dodecanedioic acid by isolated rat livers. *Bull. Math. Biol.* **67**:547–561 (2005).
17. P. Webb. The physiology of heat regulation. *Am. J. Physiol.* **268**:R838–R850 (1995).
18. E. L. Robinson, V. H. maria-Pesce, and C. A. Fuller. Circadian rhythms of thermoregulation in the squirrel monkey (*Saimiri sciureus*). *Am. J. Physiol.* **265**:R781–R785 (1993).
19. J. F. Gillooly, J. H. Brown, G. B. West, V. M. Savage, and E. L. Charnov. Effects of size and temperature on metabolic rate. *Science* **293**:2248–2251 (2001).
20. C. M. Blatteis. Prostaglandin E2: a putative fever mediator. In Mackowiak (ed.), *Fever: Basic Mechanisms and Management*, Raven Pr, 1997.
21. C. M. Blatteis and E. Sehic. Cytokines and fever. *Ann. N.Y. Acad. Sci.* **840**:608–618 (1998).
22. A. I. Ivanov and A. A. Romanovsky. Prostaglandin E2 as a mediator of fever: synthesis and catabolism. *Front. Biosci.* **9**:1977–1993 (2004).
23. D. E. Mager, E. Wyska, and W. J. Jusko. Diversity of mechanism-based pharmacodynamic models. *Drug Metab. Dispos.* **31**:510–518 (2003).
24. A. H. Jazwinski. *Stochastic Processes and Filtering Theory.* Academic, New York, 1970.
25. B. Sallstrom, S. A. Visser, T. Forsberg, L. A. Peletier, A. C. Ericson, and J. Gabrielsson. A pharmacodynamic turnover model capturing asymmetric circadian baselines of body temperature, heart rate and blood pressure in rats: challenges in terms of tolerance and animal-handling effects. *J. Pharmacokinet. Pharmacodyn.* **32**:835–859 (2005).
26. S. L. Beal and L. B. Sheiner. *NONMEM User's Guides.* NONMEM Project Group, University of California, San Francisco, 1994.
27. S. Dalai and D. S. Zhukovsky. Pathophysiology and management of fever. *J. Support Oncol.* **4**:9–16 (2006).
28. M. O. Karlsson, S. L. Beal, and L. B. Sheiner. Three new residual error models for population PK/PD analyses. *J. Pharmacokinet. Biopharm.* **23**:651–672 (1995).